❒   1785

Maximum Power Point Tracking for a Grid Connected Photovoltaic System Using Sliding Mode Control

D. Sattianadan[1], V. Kalyanasundaram[2], S. Vidyasagar[3], Deepak Kumar Nayak Roopam Jha[4]
Departement of Electrical and Electronics Engineering, SRM University, India

Article Info	ABSTRACT
	This paper presents a method to track the maximum power point for an isolated grid connected photovoltaic system. The method used to achieve this goal is sliding mode control. A high frequency flyback converter topology working in continuous conduction mode is used to boost the voltage and also provides galvanic isolation between input and output side. An inverter is used to invert the power for a grid connected operation. Therefore, the primary objective of this study is to design a sliding mode controller which can track maximum power driving a high frequency flyback converter and demonstrate its practicality as a highly efficient maximum power point tracker. This system is modelled and tested in MATLAB SIMULINK. To verify the results a practical implementation of sliding mode controller with high frequency flyback transformer is performed in a hardware setup.

Corresponding Author:

D. Sattianadan,
Departement of Electrical and Electronics Engineering,
SRM University,
Kattankulathur, Tamil Nadu.603203
Email: sattia.nadan@gmail.com

1. INTRODUCTION

Most of the world's electricity demand is fulfilled by fossil fuels and nuclear plant and very small amount is met through renewable energy resources such as photovoltaic or solar energy. Due to increase in pollution from the conventional plants and depleting sources has led to increase use of photovoltaic energy as a source of electricity. But the success of a PV plant depends on weather conditions because the output of a solar cell depends on solar irradiation and temperature which are not constant and changes with time and season. There are various conventional methods to track maximum power point such as perturb and observe (P&O) and incremental conductance. The P&O algorithm is the simplest algorithm and is easy to implement among all the algorithms. It tracks the MPP by measuring the rate of change of power with respect to voltage at every point, being zero at the MPP, positive on the left of the MPP, and negative on the right. But it has various disadvantages, such as poor tracking, less efficient during changing weather conditions, inability to track MPP during low irradiance, oscillations around MPP and slow response [1]. Incremental conductance shows better performance than P&O algorithm and track MPP by comparing the incremental and instantaneous conductance with less oscillation around MPP and faster response [2]. Fuzzy logic does not require an accurate mathematical model and can work with inexplicit input. It can also handle non-linearity in a system. It mainly has four basic step fuzzyfication , rule base, inference engine and De-Fuzzyfication. The output of FLC is the reference voltage which is generated by the change in voltage and change in current at a sampling time K from the solar panel. The reference voltage in turn generates the error signal, based on which duty cycle is generated. The only disadvantage of the FLC is that it is very difficult to formulate the

Fuzzy rules [3]. In literature [4], MPP was tracked using ANN along with hill climbing technique which helps in the reduction of oscillation around the MPP and generates the duty cycle for a boost converter.

In literature [5-6] two techniques are discussed, one is Genetic Algorithm and the other is Particle Swarm Optimization. These two techniques are used to track the MPP in partial shadow condition and then a comparison is made between both the techniques. Sliding mode control [7-9], on the other hand is one of the most effective robust control techniques for non linear and discontinuous systems due to its simplicity, stability, higher flexibility in design procedure and great performance. Due its advantages SMC has found applications in various fields such as robotics, motor control [10] and converter output control [11-12]. Flyback converter can be used with different DC link capacitor configurations. First configuration is DC link capacitors in between the DC-DC flyback converter which can boost the DC voltage to the levels compatible with the grid voltage and an inverter. But this configuration creates problem in maintaining the efficiency at high frequency [13-14]. In these mentioned literature, SMC is used to track the MPP from a PV panel which can drive a flyback converter. This paper approaches a simple method of extracting maximum power from a PV system using SMC which drives a flyback converter and then inverting the voltage for grid connected operation. The flyback converter is the lowest cost converter among isolated topologies since it uses least number of components. This mentioned topology eliminates the need of bulky and costly energy storing inductor and therefore results in the reduction of cost and size of the converter. It incorporates a high frequency transformer capable of boosting the dc voltage up to 10- 20 times depending upon the no of turns chosen which is more than that of a BOOST converter which is capable of boosting only twice the input voltage.

2.   PROPOSED SCHEME

Figure 1 shows the block diagram of the proposed scheme which consists of a PV panel as an input. To track the maximum power point of the PV panel sliding mode controller is used instead of using any MPPT algorithm. A flyback converter operating in continuous mode (CCM) is used to boost the output of the PV panel. Flyback converter can be used in both CCM and DCM mode and depending on the requirement the mode is selected. There are several advantages of selecting of DCM operation [15, 16] like it has zero-current turn on for the switches, it provides very fast dynamic response and a stable operation in all conditions, it does not exhibit reverse recovery problem and hence complications like noise, electromagnetic interference problems, and additional losses are eliminated, it does not exhibit any turn on losses and also DCM mode leads to small size of the transformer. The only disadvantages of DCM mode is that it imposes high current stress which results in decreased converter efficiency and high current ripple makes filter design difficult [17]. Whereas CCM mode has higher efficiency, easy filter design, lower primary and secondary rms current factor, smaller sized output capacitor and lower ripple current, peak mosfet and diode current. When constant current is required at the output terminal DCM mode is preferred and when constant voltage is required at the output CCM mode is preferred [18]. In this work constant voltage is the basic requirement at the output side of the converter and hence flyback converter operating in CCM mode for this work.
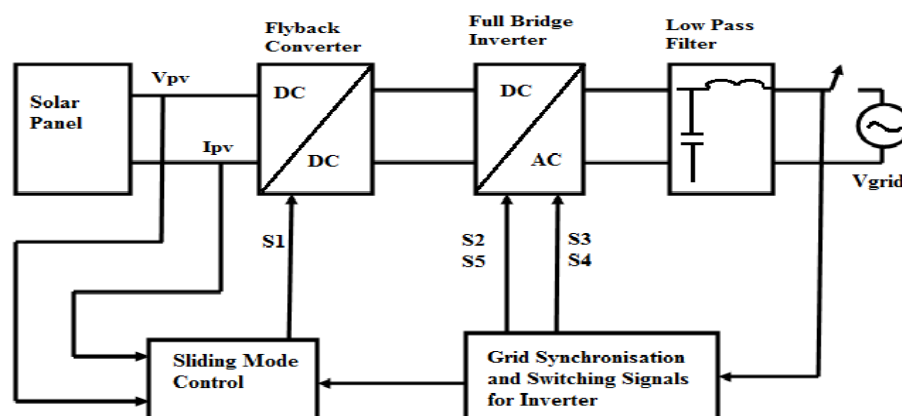

Figure 1. Block diagram of the proposed grid-connected PV inverter system based on SMC and flyback converter topology

As shown in Figure 2, the PV source is applied to a flyback converter through a decoupling capacitor. Flyback converter incorporates a metal–oxide–semiconductor field-effect transistor (MOSFET) for switching at the primary side, a high frequency flyback transformer, and a diode and a capacitor at the secondary side. This model also includes a full-bridge inverter and a low-pass filter for proper interface with the grid [19].
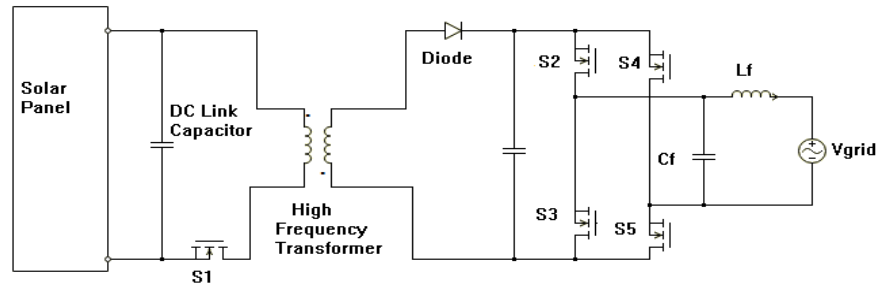

Figure 2. Circuit schematic of the proposed PV inverter system based on flyback converter topology

The proposed scheme has 5 switches one switch controls the flyback converter and the remaining 4 switch controls a Full-bridge inverter. The switching signal for S1 comes from sliding mode control and the switching signal for the remaining switches comes from the grid synchronisation and signal generation block which incorporates a sinusoidal pulse width modulation technique. SPWM takes real time reference signal from a reference system and generates signal pulse for the MOSFETS of inverter. Reference system for the proposed model is the grid from which a reference signal operating at 50 Hz is taken and is compared with a high frequency triangular carrier wave which generates the switching signal for inverter switches. The frequency of the carrier wave chosen for this work is 10 KHz.
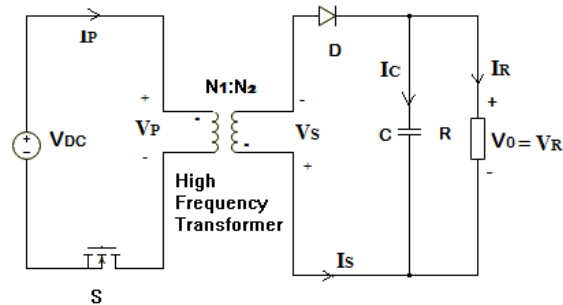

Figure 3. Circuit representation of a flyback converter

Figure 3 shows the circuit diagram of a simple flyback converter with a DC source connected to the high frequency transformer though a switch S. Transfer function of the converter can be determined as follows [18].When switch is on DC source is directly applied to the primary of the transformer. Hence,

$$V_P = V_{DC} \tag{1}$$

Since the primary and secondary are of apposite polarity, when switch is off

$$V_P = -V_0 / n \tag{2}$$

Where V_0 is the output voltage and n is the turns ratio.
        Now, average voltage across an inductor is always zero, hence

$$V_P(t) = 0 \tag{3}$$

$$V_{DC}*T_{ON} - \frac{V_0}{n}*T_{OFF} = 0 \qquad (4)$$

Where T_{ON} and T_{OFF} is the on and off time of the switch.

Substituting the value of T_{ON} and T_{OFF}

$$V_{DC} * D * T_S - \frac{V_0}{n}(1 - D) * T_S = 0 \qquad (5)$$

Where D is the Duty cycle and T_S is the switching time period.

$$V_0 = \frac{n*V_{DC}*D}{1-D} \qquad (6)$$

According to law of Conservation of Energy input power should be equal to output power

$$Pin = Pout \qquad (7)$$

$$R_{PV} = \frac{(1-D)^2}{n^2 D^2} * R_{out} \qquad (8)$$

3. CONVERTER DESIGN

The first step in the design procedure is the selection of switching frequency for the power supply. High frequency switching leads to a lower primary inductance and smaller output capacitors than the converter with lower switching frequency. However, higher switching frequency has several disadvantages like it increases switching losses leading to the decrease in the converter's efficiency and thermal performance. Taking all this point under consideration switching frequency is selected to be 50 KHz. The next step would be calculation of turns ratio of the high frequency transformer. The value of turns ratio is selected so as to regulate the duty cycle to a maximum of 50% (D_{lim}). The reason of limiting the duty cycle is that the stress on the rectifying diode and output capacitors is reduced. Turns ratio can be computed using the following equation,

$$N_{PS} = \frac{V_{IN\,min} * D_{lim}}{(V_{out} + V_D) * (1 - D_{lim})} \qquad (9)$$

Where NPS is the turns ratio, V_{INmin} is the minimum input voltage V_{out} is output voltage of converter and V_D is the diode voltage of the rectifying diode.

Duty cycle in CCM mode can be estimated by using the equation (9) as:

$$D_{CCM} = \frac{(V_{out} + V_D) * N_{PS}}{V_{IN} + (V_{OUT} + V_D) * N_{PS}} \qquad (10)$$

The next important specification to be selected for the transformer is the primary inductance. When specifying the inductance two main components to be considered are the current ripple and the RHPZ. Current ripple decreases when the inductance value is high leading to the reduction of EMI and noise. However, physical size of the transformer increases with increased value of inductance. Hence, to choose the inductance value one method can be adopted to limit the current ripple to a percentage of the average current through the primary winding during the on time of the switch. A compromise between the size and efficiency is achieved with a ripple percent (RIP%) between 60% to 90%. The average primary current can be calculated using:

$$I_{Pavg} = Ripp\% * \frac{V_{out} * I_{out}}{V_{IN\,max} * D_{min}} \qquad (11)$$

Where V_{out} and I_{out} is the output voltage and output current of the converter and D_{min} the minimum duty cycle.

Using the average primary current primary inductance can be computed as:

$$L_P = \frac{V_{IN\max} * D_{\min}}{I_{Pavg} * f_{sw}}$$

(12)

Where f_{SW} is the switching frequency of the transformer.

Secondary inductance depends upon the primary inductance and turns ratio and can be computed as:

$$L_S = \frac{L_P}{N_{PS}{}^2}$$

(13)

The capacitor connected on the secondary side of the converter is selected taking two points into consideration one is the ripple voltage and other is how the supply responds to a large change in load current. The output capacitor should be able to supply the output current when the input switch is on and current is flowing through the primary winding. The minimum value of output capacitance can be calculated as:

$$C_{out} > \frac{I_{out} * D_{\max}}{V_{ripple} * f_{sw}}$$

(14)

4.   SLIDING MODE CONTROLLER

The SMC-MPPT algorithm is divided into two steps [7]. The first step is to estimate the actual reference voltage (VMPP) value at which the system will reach its maximum power point. And the second step is to regulate the PV voltage at the VMPP voltage value. Hence, sliding surface has basically two parts. One is the reaching surface and the other is the following surface. These two mentioned step lead to a PV MPP controller working.

The main objective is that the voltage reference estimator generates a command signal and feeds it to the controller which forces the system to work at the maximum power point (MPP). The command signal is based on the difference between the PV voltage and the estimated reference voltage (VP-Vref). Using this command signal SMC generates switching signal for the converter switch. Sliding mode controller works on sliding surface such that if system state is on sliding surface, it is driven to zero. The designed controller must bind the system to remain on sliding surface. The sliding variable for this work is defined as:

$$S = e = VPV - Vref$$

(15)

$$U = \frac{1}{2}(1 + sign(s))$$

(16)

$$U = 1 \text{ when } S > 0$$
$$= 0 \text{ when } S < 0$$

(17)

Stability of SMC can be demonstrated using Lyapunov theory. A positive function is defined by:

$$V = \frac{1}{2}S2 > 0$$

(18)

Taking the time derivative of eq (36), we get:

$$\frac{dV_{PV}}{dt} = S * \frac{dS}{dt}$$

(19)

Taking the time derivative of eq (19), we get:

$$\frac{dS}{dt} = \frac{de}{dt} = \frac{dV_{PV}}{dt}$$

(20)

Based on Lyapunov theory when V is positive and its time derivative is positive semi definite, then the system is asymptotically stable. For the system, used in this paper, when S = 0 then system is stable and the desired voltage is achieved and maximum power point is reached. When S > 0, switch S1 is open and duty cycle is increased.

$$\frac{dV_{PV}}{dt} < 0 \text{ and } \frac{dS}{dt} < 0, \text{ hence } S*\frac{dS}{dt} < 0$$

When S < 0, switch S1 is closed and duty cycle is decreased. If duty cycle decreases, RPV increases and thus I_{PV} decreases and V_{PV} increases. As the change in voltage is in positive direction, we get:

$$\frac{dV_{PV}}{dt} > 0 \text{ and } \frac{dS}{dt} > 0, \text{ hence } S*\frac{dS}{dt} < 0$$

5.   SIMULATIONS RESULTS

A prototype circuit of the proposed controller at rated power was built, to evaluate its real-time performance as shown in Figure 4. The major components and their specifications used in the hardware setup are listed in Appendix. The PV panel used as input to the setup was able to supply a voltage of 20 V and a current of 6 A to the converter in a bright sunny day with a very high temperature as shown in the Figure 5. As a result the total input power is 120 W. Figure 6 shows the primary and secondary voltage of the flyback converter. As the converter is operating in CCM mode the voltage waveforms are square pulses. The input voltage to the converter is 20 V as shown in the Figure 6(a). The time period of the waveforms is 20μsec that proves the converter is working at switching frequency of 50 KHz. The converter is able to boost the input voltage to 300 V as shown in the Figure 6(b) having vertical scale of 10 V/div and probe multiplication factor of 10 V/div with a efficiency of 96%. The secondary voltage waveform is not a square pulse because of the transformer losses occurring during the process.

Figure 7 shows the inverted voltage and current waveforms of the designed model. Figure 7(a) shows the voltage waveform of inverter output without filter having high level of harmonics. Figure 7(b) shows the filtered waveforms of voltage and current which is grid interfaced with a power factor of 0.99. The peak value of the AC voltage is 320 V and AC current is 0.8 A respectively hence producing the rms voltage of more than 220V and rms current of 0.5 A. The overall efficiency of the model is more than 90%.
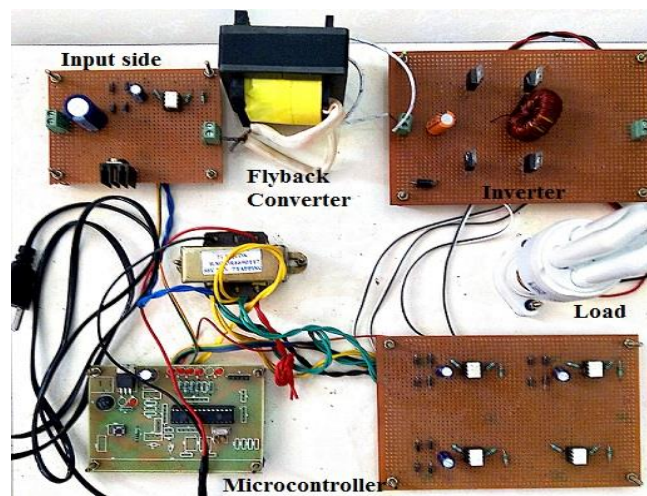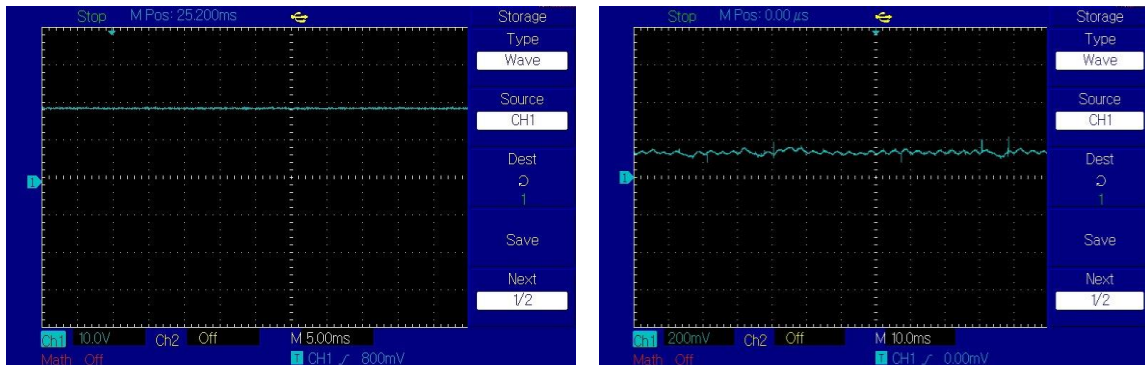

Figure 4. Experimental setup of the proposed scheme

Figure 5. Experimental waveforms of PV voltage and current. Vertical scale: 10 V/div and 20 A/div. Horizontal scale: 10msec
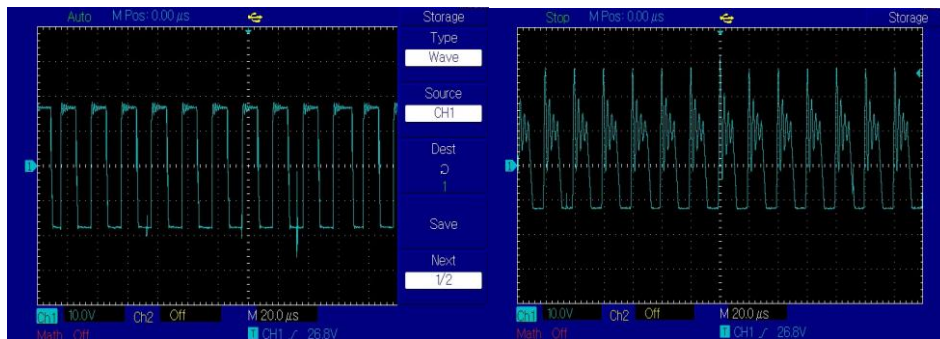

Figure 6. Experimental waveforms of the flyback converter (a) primary voltage (b) secondary voltage, vertical scale: 10 V/div and horizontal scale: 20 µsec
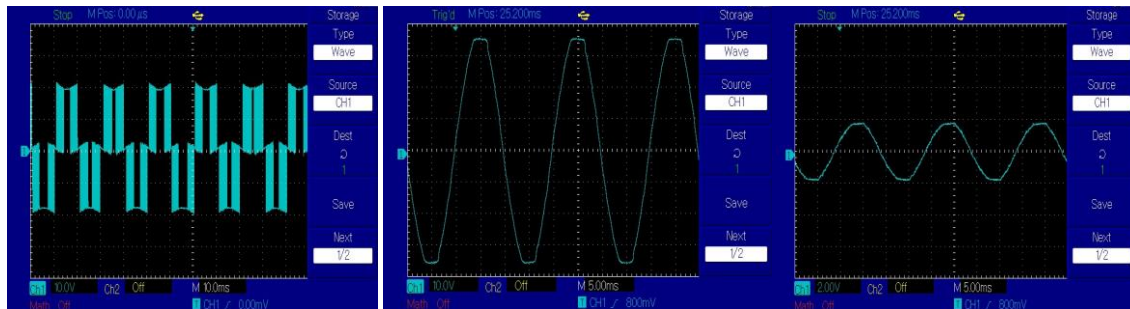

Figure 7. (a) Grid voltage without filter (b) grid voltage and current with filter. Vertical scale: 10 V/div and 1 A/div. Horizontal scale: 5msec

6. CONCLUSION

A single phase grid connected MPPT technique for a PV system based on flyback topology has been successfully designed and implemented using sliding mode control. A low power PV panel with maximum voltage of 36 V can be used to produce grid interfaced voltage and current using the flyback converter. Maximum power point has been tracked effectively using SMC with an efficiency of 97%. Flyback topology boosted the PV panel voltage with an efficiency of 96%. Hardware results obtained confirmed that the proposed scheme can be used for low power applications of PV panel in grid connected mode and was able to produce grid synchronised voltage and current with a power factor 0.99.

APPENDIX

Design parameters	Specification
PV model	230 Wp – 24 v
Maximum power from PV panel	230W
Open circuit voltage	43.97 V
Short circuit current	7.14 A
Maximum PV voltage	35.40V
Maximum PV current	7.14 A
Converter input voltage	16 V- 36 V
Converter output voltage	350 V
Switching frequency	50 kHz
Time period	20 μsec
Ton	8 μsec

REFERENCES

[1] J. Surya Kumari and Ch. Saibabu. "Maximum Power Point Tracking Algorithms for Grid- Connected Photovoltaic Energy Conversion System". *International Journal of Power Electronics and Drive System (IJPEDS).* Vol. 3, No. 4, December 2014, pp. 424~437

[2] Zakzouk NE, Abdelsalam AKA, Helal A, Williams BW. "Modified variable-step incremental conductance maximum power point tracking technique for photovoltaic systems". *39th Annual conference of the IEEE industrial electronics society. IECON;* 2013. pp. 1741–8.

[3] Narendiran.S, Sarat Kumar Sahoo, Raja Das, Ashwin Kumar Sahoo. "Fuzzy logic controller based maximum power point tracking for PV system". *3rd International Conference on Electrical Energy Systems (ICEES)* 2016. pp. 29-34.

[4] K. Ranjani, M. Raja, B. Anitha. Maximum Power Point Tracking by ANN Controller for a Standalone Photovoltaic System: International Journal of Electrical, Computer, Energetic, Electronic and Communication Engineering Vol: 8, No: 3, 2014.

[5] Afef Badis, Mohamed Nejib Mansouri, Anis Sakly. "PSO and GA-based maximum power point tracking for partially shaded photovoltaic systems": *7th International Renewable Energy Congress (IREC)* 2016. pp. 1-6.

[6] A. H. ALQahtani, V. I. Utkin. "Control of Photovoltaic System Power Generation Using Sliding Mode Control" *IEEE International Conference on Power System Technology (POWERCON)* 2012. pp. 1-12

[7] Maissa Farhat , Oscar Barambones , Lassaad Sbita. "A new maximum power point method based on a sliding mode approach for solar energy harvesting" *The 7th International Conference on Applied Energy ICAE2015.* pp. 361 – 366

[8] Yan Ping Jiao and Fang Lin Luo. "An Improved Sliding Mode Controller for Boost Converter in Solar Energy System". *4th IEEE Conference on Industrial Electronics and Applications ICIEA* 2009 pp. 805-810.

[9] B. Khiarp, A. Sellamp, R. Andoulsp, R. Mhiri and M. Ksouri. "Discrete control by Sliding Mode of a Photovoltaic System". *First International Symposium on Control Communications and Signal Processing* 2004. pp 469-474.

[10] Jagat Jyoti Rath, Suman Saha and Hanumath Prasad Ikkur. "Sliding Mode Scheme For Speed And Current Control Of Brushless DC (BLDC) Motor". *IEEE-International Conference on Advances In Engineering, Science And Management (ICAESM)* 2012. pp.450-455.

[11] Hafiz Kashif Iqbal and Dr. Ghulam Abbas. "Design and Analysis of SMC for Second Order DC-DC Flyback Converter" *17th IEEE International Multi Topic Conference* 2014. pp 533-538.

[12] Amir Hussain, Avanish Kumar and Laxmidhar Behera. "Sliding mode control of a buck converter for maximum power point tracking of a solar panel" *IEEE International Conference on Control Applications (CCA) , August 2013.* pp. 661-666.

[13] Lallu mol K Johny, Jose Sebastian T.K. "A Flyback DCM DC-AC Converter for PV Applications". *Annual International Conference on Emerging Research Areas and International Conference on Microelectronics, Communications and Renewable Energy, 2013.* pp 1-6.

[14] Bunyamin Tamyurek and Bilgehan Kirimer." An Interleaved High-Power Flyback Inverter for Photovoltaic Applications" *IEEE transaction on Power Electronics*, Vol. 30, NO. 6, June 2015.

[15] Kai YAO, and Xiaoyong FU Jianguo Lv. " DCM Flyback PFC Converter with Optimum Utilization Control of Switching Cycles" *IEEE Energy Conversion Congress and Exposition (ECCE),*2015. pp. 2445-2452.

[16] A. Ch. Kyritsis, E. C. Tatakis and N. P. Papanikolaou. "Optimum Design of the Current-Source Flyback Inverter for Decentralized Grid-Connected Photovoltaic Systems" *IEEE Transactions on Energy Conversion* Vol. 23, No. 1, March 2008. pp. 281-293.

[17] S. Howimanpom and C. Bunlaksananusom. "Performance Comparison of Continuous Conduction Mode (CCM) and Discontinuous Conduction Mode (DCM) Flyback Converters" *The Fifth International Conference on Power Electronics and Drive Systems, 2003. PEDS* 2003. pp. 1434-1438.

[18] Simon Ang and Alejandro Oliva. " Power- Switching Converters". Taylor & Francis published in 2005.

[19] Haibing Hu, Souhib Harb, Dehua Zhang, Qian Zhang, Z. John Shen, and Issa Batarseh. "A Three-port Flyback for PV Microinverter Applications With Power Pulsation Decoupling Capability*" IEEE Transaction on Power Electronics*, Vol. 27, NO. 9, September 2012.